Journal of Alloys and Compounds 620 (2015) 376–382

Contents lists available at ScienceDirect

Journal of Alloys and Compounds

journal homepage: www.elsevier.com/locate/jalcom

Targeted structural changes and magnetic properties study in $(Ho/Er)_5Ga_{3-x}(Co/Fe)_x$

Fang Yuan [a], Alex V. Morozkin [b], Yurij Mozharivskyj [a,*]

[a] Department of Chemistry and Chemical Biology, McMaster University, 1280 Main Street West, Hamilton, Ontario L8S 4M1, Canada
[b] Department of Chemistry, Moscow State University, Leninskie Gory, House 1, Building 3, GSP-2, Moscow 119992, Russia

ARTICLE INFO

Article history:
Received 14 July 2014
Received in revised form 18 September 2014
Accepted 21 September 2014
Available online 14 October 2014

Keywords:
Rare-earth alloys
Crystal structure
Magnetic transition
Magnetocaloric effect

ABSTRACT

Phase transformations in the $Ho_5Ga_{3-x}Co_x$ ($x = 0$, 0.1, 0.2, 0.3, 0.4, 0.5, 1), $Er_5Ga_{3-x}Fe_x$ ($x = 0$, 0.4), and $Er_5Ga_{3-x}Co_x$ ($x = 0$, 0.4) system reveal an intimate coupling between the crystal structure and atomic size. A decrease in the effective atomic size of the Ga site through the transition metal substitution results in a transition from the Mn_5Si_3-type structure to Cr_5B_3-type one. According to the single crystal X-ray diffraction, Co and Fe substitution occurs only on the Ga 8*h* site. The relationship between the composition, crystal structures and magnetic properties is analyzed. Magnetization studies for pure Ho_5Ga_3, $Ho_5Ga_{2.9}Co_{0.1}$, $Ho_5Ga_{2.7}Co_{0.3}$, $Ho_5Ga_{2.6}Co_{0.4}$ phases reveal an antiferromagnetic ordering for Ho_5Ga_3, but ferromagnetic transition for the other phases. In addition, the ferromagnetic transition temperature increases with the Co amount. The maximum magnetic entropy change of −12.7 J/kg K is obtained in $Ho_5Ga_{2.6}Co_{0.4}$ at 32.5 K.

1. Introduction

Increasing environmental pressure and limited natural resources urge development of novel, more efficient cooling techniques that can replace conventional vapor-cycle refrigeration. One of the most promising approaches is magnetic refrigeration based on magnetocaloric effect (MCE). However, some important problems have to be addressed prior to the implementation of this technique. One of the most challenging tasks is to achieve large MCE values in relatively small magnetic fields. A breakthrough was the discovery of a giant magnetocaloric effect (GMCE) in $Gd_5Si_2Ge_2$ in 1997 [1]. This material undergoes a first-order coupled magneto-structural transition and the total entropy change includes not only a magnetic entropy contribution, but also a structural one.

The discovery of a GMCE in $Gd_5Si_2Ge_2$ initiated extensive research on the related RE_5T_4 phases (*RE* is a rare earth, *T* is a *p*-element). One of the important outcomes is the possibility to tune the structural and magnetic properties of RE_5T_4 through valence electron concentration (VEC) [2–6]. It was also shown that the VEC stabilization can be applied to other phases, e.g. the non-existing Gd_4Ge_3 binary can be stabilized through a VEC increase [7].

Comparing with the RE_5T_4 series, the magnetic and structural properties of RE_5X_3 (*X* is Si, Ge, Sn, Sb, Bi) are less systematically explored, and in general the factors governing their stability and phases transformations are not as well understood. The literature data suggest that both the RE_5X_3 tetralides and pnictides adopt the Mn_5Si_3-type structure, suggesting that neither the VEC nor atomic size itself dictates their stability [8–11]. On the other hand, the RE_5Ga_3 phases present an interesting case as their structures are governed by the size of the rare earths. The three structures identified for RE_5Ga_3 are hexagonal Mn_5Si_3-type, tetragonal Cr_5B_3-type and W_5Si_3-type ones (Fig. 1), and their stability can be summarizes as follows (except for La and Y): (1) a hexagonal Mn_5Si_3-type structure ($P6_3/mcm$) forms for Ho (1.74 Å) and smaller rare-earth atoms; (2) a tetragonal Cr_5B_3-type structure ($I4/mcm$) is stable between Dy (1.75 Å) and Nd (1.81 Å); (3) a tetragonal W_5Si_3-type structure ($I4/mcm$) is observed for Pr (1.82 Å) and Ce (1.83 Å); (4) RE_5Ga_3 phases are unknown for Yb (1.94 Å) and Eu (2.00 Å) [12–17]. This structure-atomic size relationship provides a possibility to stabilize a specific structure of RE_5Ga_3 through elemental substitution either on the *RE* or Ga sites. Since Ho_5Ga_3 and Er_5Ga_3 sit close to the Cr_5B_3–Mn_5Si_3 boundary, a transition between the two structures should be achieved by tuning the average atomic size of the *RE* or Ga sites.

In our research, we focused on the $Ho_5Ga_{3-x}Co_x$, $Er_5Ga_{3-x}Fe_x$, and $Er_5Ga_{3-x}Co_x$ systems as the size difference between Co (Fe) and Ga ($r_{Fe} = 1.24$ Å, $r_{Co} = 1.25$ Å and $r_{Ga} = 1.26$ Å) is comparable to that between the rare-earth elements ($r_{Er} = 1.73$ Å, $r_{Ho} = 1.74$ Å and $r_{Dy} = 1.75$ Å) and, in principle, should allow structural tuning.

* Corresponding author.

http://dx.doi.org/10.1016/j.jallcom.2014.09.158
0925-8388/

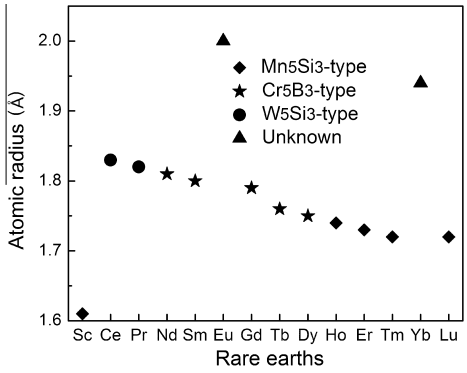

Fig. 1. Structural map for RE_5Ga_3 phases.

Table 1
Structure types of the major phase in $Ho_5Ga_{3-x}Co_x$, $Er_5Ga_{3-x}Fe_x$, and $Er_5Ga_{3-x}Co_x$.

Sample	Treatment	Str. type of major phase
Ho_5Ga_3	Cast	Mn_5Si_3
	Annealed	Ba_5Si_3
$Ho_5Ga_{2.9}Co_{0.1}$	Cast	Mn_5Si_3
	Annealed	Ba_5Si_3
$Ho_5Ga_{2.8}Co_{0.2}$	Cast	$Mn_5Si_3 + Cr_5B_3$
	Annealed	Cr_5B_3 + impurity/ies
$Ho_5Ga_{2.7}Co_{0.3}$	Cast	$Mn_5Si_3 + Cr_5B_3$
	Annealed	Cr_5B_3
$Ho_5Ga_{2.6}Co_{0.4}$	Cast	$Mn_5Si_3 + Cr_5B_3$
	Annealed	Cr_5B_3
$Ho_5Ga_{2.5}Co_{0.5}$	Cast	$Mn_5Si_3 + Cr_5B_3$
	Annealed	Cr_5B_3 + impurity/ies
Ho_5Ga_2Co	Cast	$Mn_5Si_3 + Cr_5B_3$
	Annealed	Cr_5B_3 + impurity/ies
Er_5Ga_3	Cast	Mn_5Si_3 + impurity/ies
	Annealed	Ba_5Si_3
$Er_5Ga_{2.6}Fe_{0.4}$	Cast	$Mn_5Si_3 + Cr_5B_3$
	Annealed	Cr_5B_3
$Er_5Ga_{2.6}Co_{0.4}$	Cast	Mn_5Si_3
	Annealed	Cr_5B_3 + impurity/ies

Additionally, the RE_5Ga_3 phases order antiferromagnetically or remain paramagnetic [14,17,29], which makes them unsuitable for magnetic refrigeration. Through the Co or Fe substitution, we aimed to change the ground magnetic state into a ferromagnetic one. In this work, we reported on the successful stabilization of the Cr_5B_3-type structure in Ho_5Ga_3 and Er_5Ga_3 via Co and Fe substitution. We also presented magnetic properties of newly discovered $Ho_5Ga_{3-x}Co_x$ series and MCE of $Ho_5Ga_{2.7}Co_{0.3}$ and $Ho_5Ga_{2.6}Co_{0.4}$ phases with the Cr_5B_3-type structure.

2. Experimental section

2.1. Synthesis

The starting materials were pieces of holmium and erbium (99.9+ wt.%, distilled grade, Metall Rare Earth Limited, China), cobalt (99.9 wt.%, Alfa Aesar), iron (99.9 wt.%, Alfa Aesar) and gallium (99.9999 wt.%, Alfa Aesar). The surface of Ho and Er metal lumps were cleaned with a file before they were cut into pieces. The $Ho_5Ga_{3-x}Co_x$ (x = 0, 0.1, 0.2, 0.3, 0.4, 0.5, 1), $Er_5Ga_{3-x}Fe_x$, and $Er_5Ga_{3-x}Co_x$ (x = 0, 0.4) samples were arc-melted at least three times to improve the homogeneity. The cast samples were wrapped in individual Ta foils, sealed in evacuated silica tubes and annealed at 900 °C for 1 week to improve crystallinity and homogeneity. The tubes were then quenched in cold water.

2.2. X-ray powder diffraction

Powder X-ray diffraction (XRD) data for the $Ho_5Ga_{3-x}Co_x$ (x = 0, 0.1, 0.2, 0.3, 0.4, 0.5, 1), $Er_5Ga_{3-x}Fe_x$, and $Er_5Ga_{3-x}Co_x$ (x = 0, 0.4) samples were collected on a PANalytical X'Pert Pro diffractometer equipped with a linear X'Celerator detector and using the Cu Kα1 radiation. The phase analysis and lattice constant refinement were carried out through the Rietveld refinement using the *Rietica* program. [18] The cast Ho_5Ga_3 and $Ho_5Ga_{2.9}Co_{0.1}$ samples contained Mn_5Si_3-type phases, however annealing at 900 °C yielded the Ba_5Si_3-type phase and unknown impurity/ies. All the other cast Ho-containing samples were found to be mixture of both Mn_5Si_3-type (main phase) and Cr_5B_3-type phases; annealing yielded high-purity Cr_5B_3-type phases only for the $Ho_5Ga_{2.7}Co_{0.3}$ and $Ho_5Ga_{2.6}Co_{0.4}$ samples. The cast Er_5Ga_3 was a mixture of the Mn_5Si_3-type phases and unknown impurity/ies. The cast $Er_5Ga_{2.6}Co_{0.4}$ and $Er_5Ga_{2.6}Fe_{0.4}$ had both Mn_5Si_3-type (main phase) and Cr_5B_3-type phases. After annealing at 900 °C for 1 week, a pure Cr_5B_3-type phase was obtained in $Er_5Ga_{2.6}Fe_{0.4}$, while large amounts of Er_3Ga_2 impurities were observed in $Er_5Ga_{2.6}Co_{0.4}$ (Table 1).

Based on the phase analysis, five high-purity samples were obtained: cast Ho_5Ga_3 and $Ho_5Ga_{2.9}Co_{0.1}$, annealed $Ho_5Ga_{2.7}Co_{0.3}$, $Ho_5Ga_{2.6}Co_{0.4}$ and $Er_5Ga_{2.6}Fe_{0.4}$. The unit cell dimensions derived from the Rietveld refinement (*Rietica* program [18]) for these samples are summarized in Table 2. The lattice parameters decrease upon the transition metal substitution due to the atomic size difference between Ga and Co/Fe.

2.3. X-ray single-crystal diffraction

Single crystal X-ray diffraction studies were performed on the crystals extracted from the cast Ho_5Ga_3, annealed $Ho_5Ga_{2.6}Co_{0.4}$, $Er_5Ga_{2.6}Co_{0.4}$ and $Er_5Ga_{2.6}Fe_{0.4}$ samples. Room-temperature data were collected on a STOE IPDSII diffractometer with Mo Kα radiation and in the full reciprocal sphere. Numerical absorption correction was based on the crystal shapes that was originally derived from optical face indexing, but later optimized against equivalent reflections using the STOE *X-shape* software [19]. Structure refinements were performed using the *SHELXL* program [20]. Crystallographic data and refinement results are summarized in Tables 3 and 4. The structure types obtained from single crystal solution agree well with the results of powder X-ray diffraction.

2.4. Electron probe microanalysis

The quantitative elemental analysis of $Ho_5Ga_{2.6}Co_{0.4}$ was performed with an INCA-Energy-350 X-ray EDS spectrometer (Oxford Instruments) on the Jeol JSM-6480LV scanning electron microscope (20 kV accelerating voltage, beam current 0.7 nA and beam diameter 50 μm). Signals averaged over three points per phase had estimated standard deviations of 1 at.% for Ho (measured by *L*-series lines), Co, and 5 at.% for Ga (measured by *K*-series lines).

2.5. Magnetometry

Magnetic measurements were performed using a Superconducting Quantum Interference Device (SQUID) on the Magnetic Property Measurement System (MPMS) magnetometer. Magnetization in a field-cooled (FC) mode for the polycrystalline Ho_5Ga_3 (cast), $Ho_5Ga_{2.9}Co_{0.1}$ (cast), $Ho_5Ga_{2.7}Co_{0.3}$ (annealed) and $Ho_5Ga_{2.6}Co_{0.4}$ (annealed) samples was measured in the 100 Oe field from 300 to 5 K. Magnetization of other samples was not measured because of the significant amounts of secondary phases. Maxima in the derivatives of the magnetization with respect to temperature were taken as Curie (T_C) temperatures. The cusp temperature on the thermal magnetization curve was taken as the Neel (T_N) temperature of Ho_5Ga_3 (cast). Weiss temperature (θ_p) and effective magnetic moment per formula unit (μ_{eff}) were obtained by fitting the paramagnetic data to the Curie–Weiss law. The magnetocaloric effect for $Ho_5Ga_{2.7}Co_{0.3}$ and $Ho_5Ga_{2.6}Co_{0.4}$ was evaluated from the magnetization vs. field (M vs. H) curves measured around the ordering temperature with 5 K steps. The magnetic field changed from 0 to 50 kOe in 2 kOe steps.

Table 2
Crystallographic data for the $Ho_5Ga_{3-x}Co_x$ and $Er_5Ga_{2.6}Fe_{0.4}$ samples determined from the powder X-ray diffraction.

Composition	Treatment	Str. type	a (Å)	c (Å)	V (Å^3)
Ho_5Ga_3	Cast	Mn_5Si_3	8.5403(1)	6.4151(2)	405.21(1)
$Ho_5Ga_{2.9}Co_{0.1}$	Cast	Mn_5Si_3	8.5339(1)	6.4086(1)	404.200(3)
$Ho_5Ga_{2.7}Co_{0.3}$	Annealed	Cr_5B_3	7.5753(1)	13.8844(3)	796.76(2)
$Ho_5Ga_{2.6}Co_{0.4}$	Annealed	Cr_5B_3	7.5674(1)	13.8514(6)	793.21(4)
$Er_5Ga_{2.6}Fe_{0.4}$	Annealed	Cr_5B_3	7.5360(1)	13.8731(5)	787.88(4)